IEA Wind Task 52 Lunch seminar

Validation of near-shore wind measurements using a dual scanning LiDAR

Yuko Ueda

Japan Wind Energy Consulting Inc.

WINC

- Offshore wind development current status in Japan
  - There is considerable interest in installing offshore wind farms in moving toward a carbon-neutral society.
  - A **new maritime renewable energy policy** has been announced by the Japanese government to stimulate the market. Under this new policy, the government-led tenders for several regions have started to materialize actual projects as of 2022.

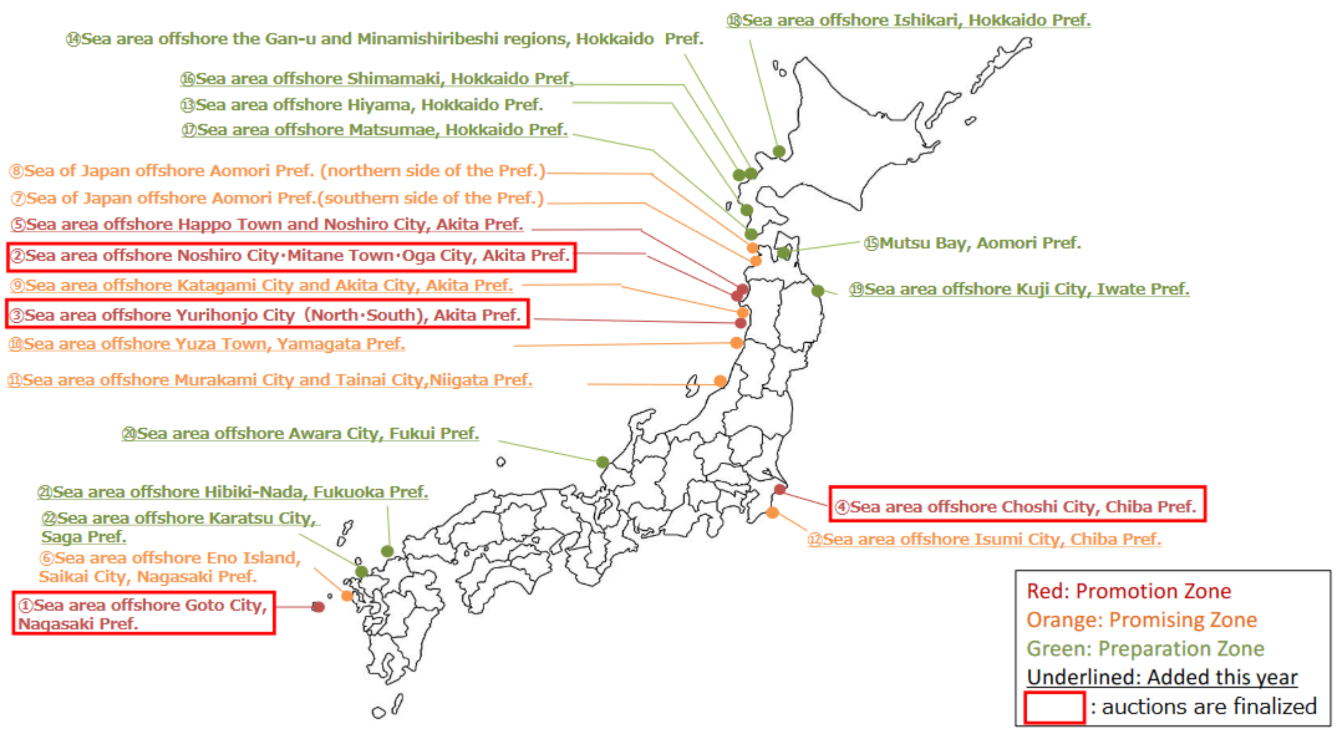

Ref: NEDO HP（https://www.nedo.go.jp/content/100949197.pdf)

Introduction [2/2]

- Offshore wind development Challenges in Japan
  - The offshore wind farm industry in Japan is currently positioned in the **early phase of installation**, and most wind farm developers are facing some challenges.
  - One issue is the **absence of accurate and economical means for assessing offshore wind resources** and **site-specific conditions**.
    - ➢ Difficult to build a met mast offshore without encountering technical, social and financial constraints.
  - Most planned offshore wind farms will be **within a few kilometers of the coastline**.
    - ➢ This reduces companies' motivation to build offshore met masts due to the unsuitable cost.
  - Wind measurement using **LiDAR** devices has received significant attention in the Japanese wind energy community. Especially, **the use of multiple LiDAR devices** is expected to be effective for measuring **not only mean wind conditions but also turbulence characteristics**.
- Measurement campaign was conducted in **NEDO project** “Establishment of offshore wind resource assessment method”

Objectives

- The objective of this study was to investigate the performance of near-shore wind measurements using a **dual scanning LiDAR system deployed near the coast** by comparing results with reference measurements obtained from an offshore met mast 60 m tall.

- The accuracy of the **10-min mean wind speed** and **direction** from the dual scanning LiDAR system was examined first, and then the accuracy of the **wind shear** and **veer** measurements, which consist of vertical profiles of wind speed and direction, was investigated by comparison with observations from a vertical profiling LiDAR device (VL).

- To that end, the difference in the **TI** obtained from **cup anemometers** and a **sonic anemometer (SA)** mounted to the offshore met mast and the **dual scanning LiDAR system** was evaluated.

Reference

Susumu Shimada, Tetsuya Kogaki, Mizuki Konagaya, Toshinari Mito, Ryuzou Araki, Yuko Ueda, Teruo Ohsawa, Validation of near-shore wind measurements using a dual scanning light detection and ranging system, 06 June 2022, https://doi.org/10.1002/we.2757

WINC

The scanning LiDAR validation campaign

- Experiments were conducted during the period November 2020 to October 2021, at a coastal research site of Mutsu–Ogawara Port, which is located on the Pacific coast of Aomori Prefecture in northern Japan.
- This study show the result of during the period November 7 to December 31, 2020.
- At this site, several validation campaigns have been conducted involving both scanning LiDAR devices and floating LiDAR systems.

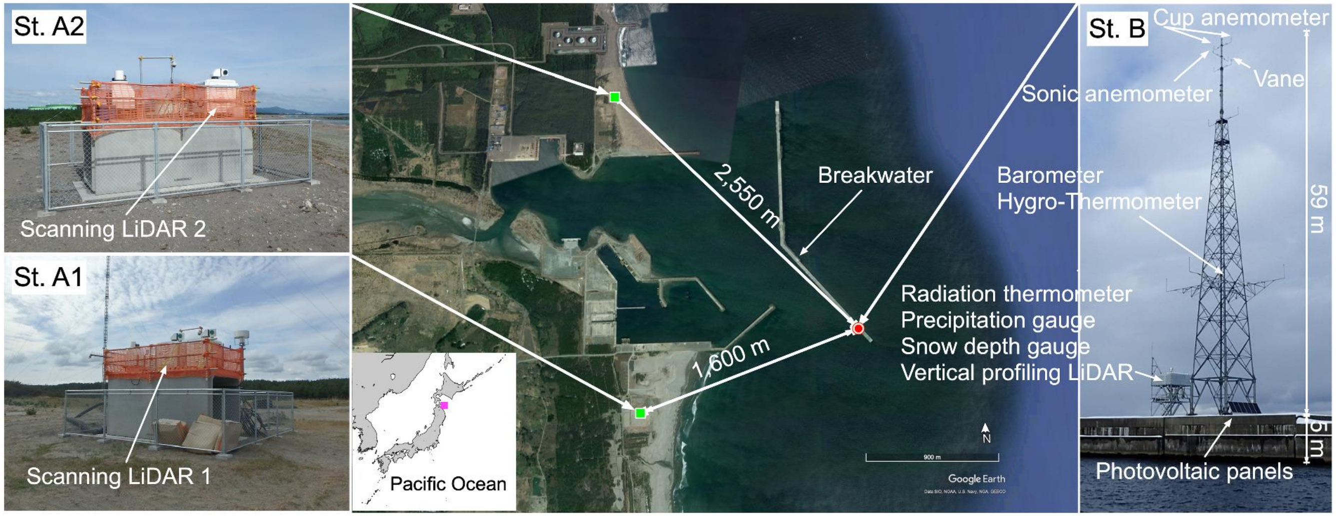

Overview of the instruments used in the experiments

Scanning LDAR configurations [1/2]

◆ Dual-Doppler virtual tower

- A Dual-Doppler virtual tower, which is a concept to virtually establish a tower by crossing a pair of laser beams at several heights, was set up.
- Figure shows the geometry of the scanning LiDAR devices, and their detailed configurations, respectively.

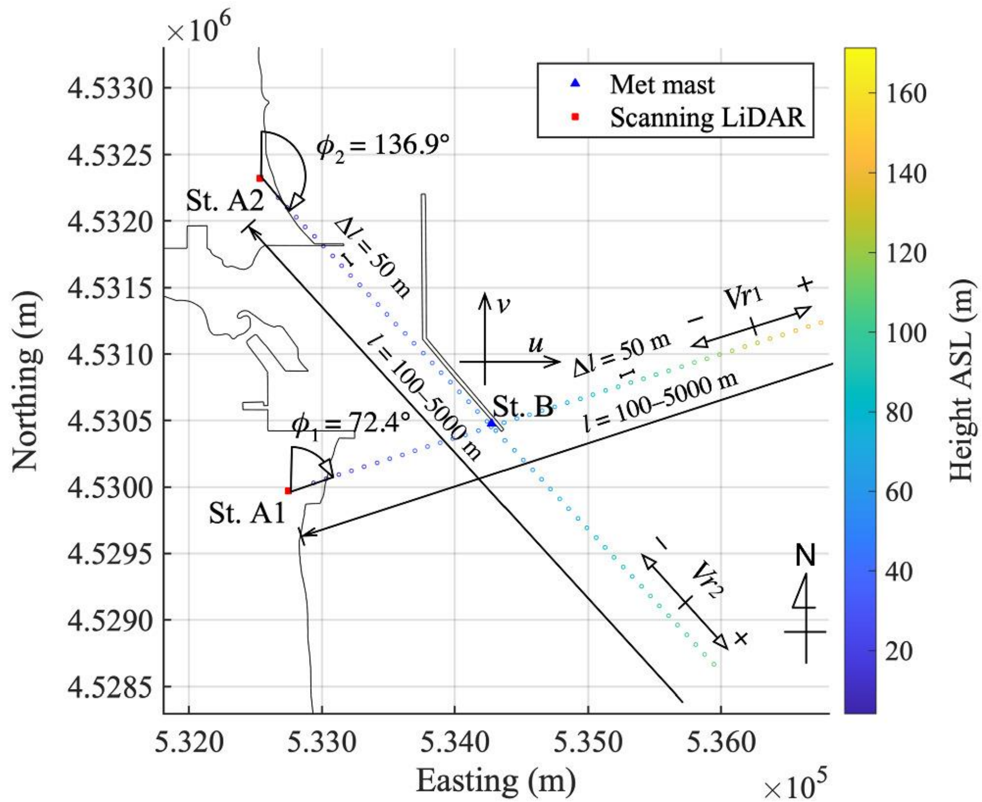

Measurement positions of radial velocities for SL 1 with an elevation angle of 2.0° and SL 2 with an elevation angle of 1.3°

Scanning LDAR configurations [2/2]

WINC

- Dual-Doppler virtual tower
  - Table shows the geometry of the scanning LiDAR devices, and their detailed configurations, respectively.
  - The devices were configured to have identical settings, except for the azimuth angle and elevation angle settings to cross the laser beams above the met mast with a crossing angle of 64.5°.

Scanning LiDAR configurations

Parameter	Scanning LiDAR 1	Scanning LiDAR 2
Model	WLS200s	WLS200s
Height	9.7 m ASL	9.3 m ASL
Azimuth angle	72.4 deg.	136.9 deg.
Elevation angle	2.0, 3.9, 6.0 deg.	1.3, 2.5, 3.0 deg.
Slant range to the met mast	1,600m	2,550m
Measurement height	66, 120, 180m ASL	66, 120, 180m ASL
Range gate length	50 m	50 m
Accumulation time	1 s	1 s
Duration for 3 level measurements	7 s	5 s
Measurement range	100 to 5000m	100 to 5000m

WINC

- The radial velocities
  - evaluating the accuracy of the radial velocity measurements by the scanning LiDAR devices by comparing them with observations from the SA mounted at a height of 61 m ASL.

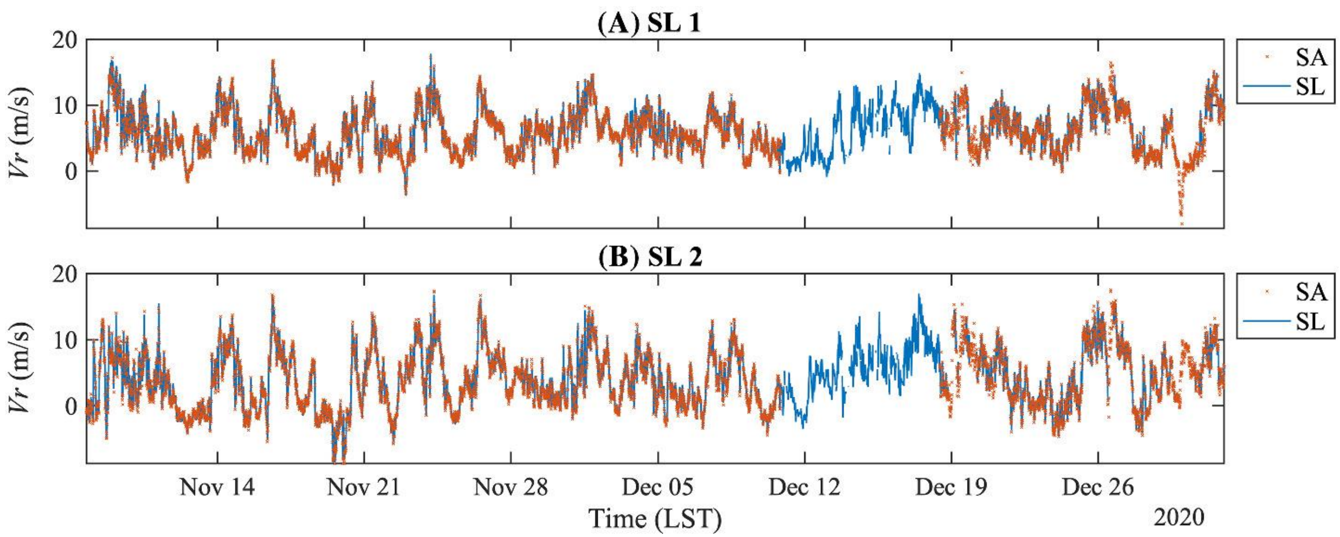

Time series of radial velocities obtained from the sonic anemometer (SA) and (A) SL 1 and (B) SL 2 for the period November 7 to December 31, 2020. The three-axis wind speeds of SA were projected to the line-of-sight direction of each scanning LiDAR device with their azimuth and elevation angles

Results - Radial velocity [1/2]

- The radial velocities
  - **biases of less than 0.2 m/s** and **coefficients of determination of more than 0.99**.

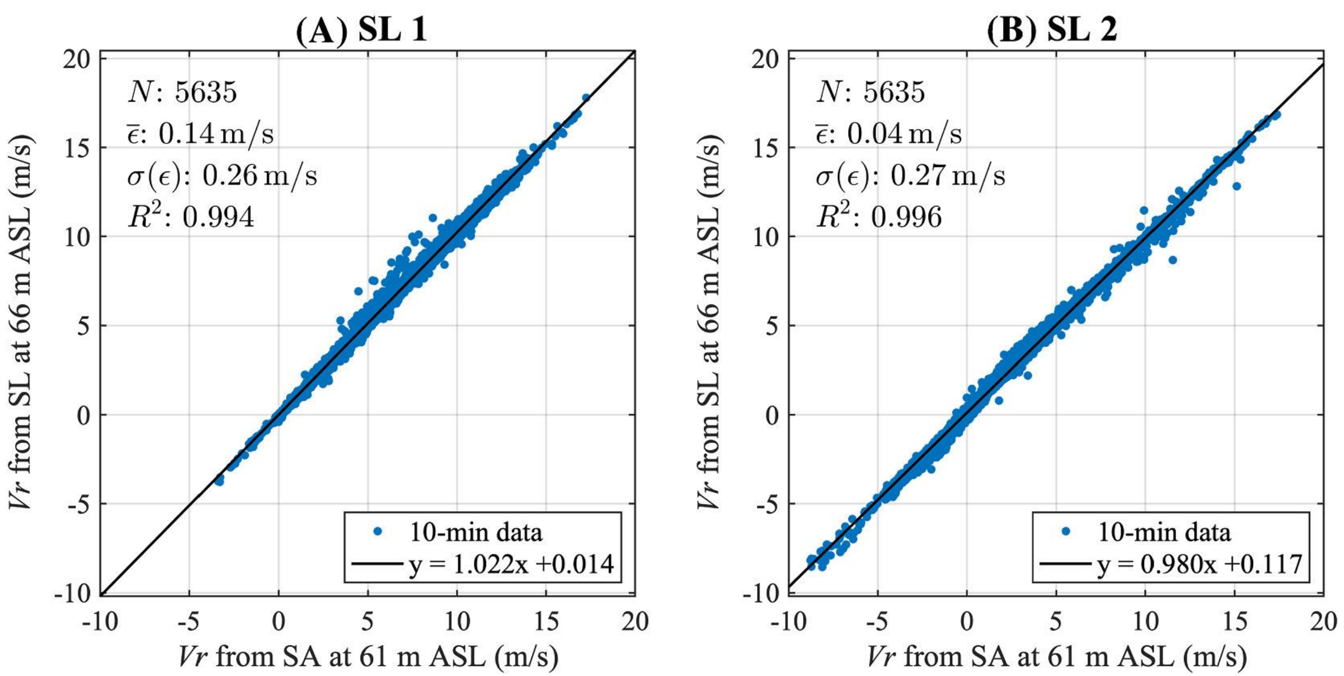

Scatter plots between the radial velocities obtained from the sonic anemometer (SA) and (A) SL 1 and (B) SL 2

Results - 10-min mean wind speed and direction [1/2]

- The 10-min mean wind speed and direction values
  - Figure shows the time series of 10-min mean wind speeds and directions obtained from the met mast and the dual LiDAR system.

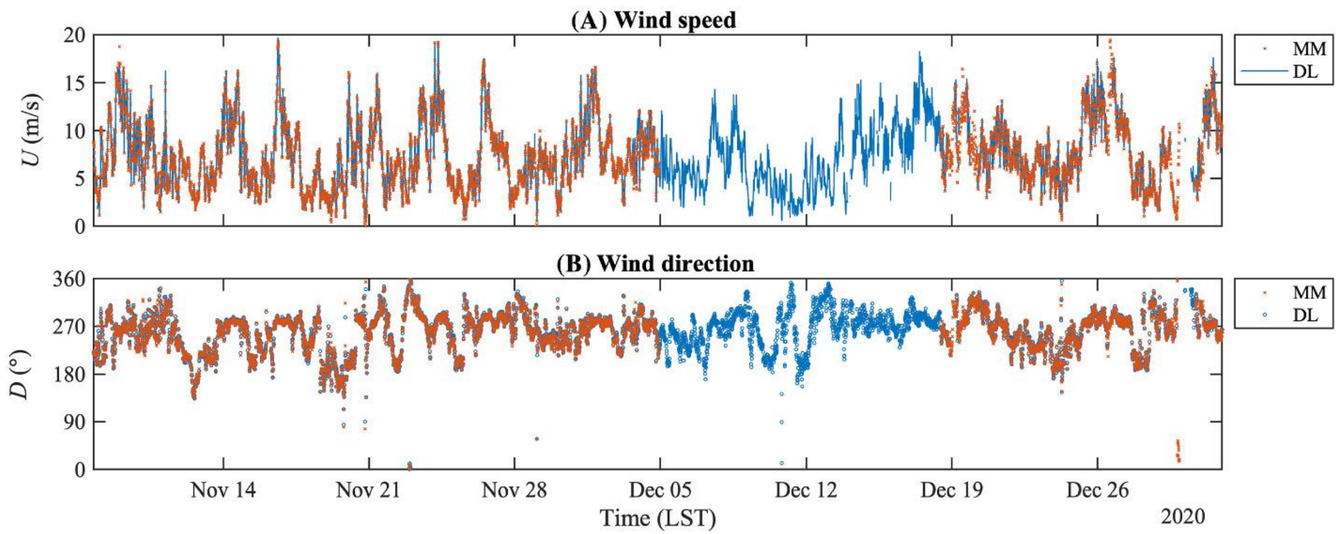

Time series of (A) 10-min mean wind speeds and (B) directions obtained from the met mast (MM) and the dual LiDAR system (DL) for the period November 7 to December 31, 2020

- The 10-min mean wind speed and direction values
  - Figure shows scatter plots of the met mast wind speeds and directions versus the dual LiDAR wind speeds and wind directions.
  - he records with wind speeds less than 2 m/s were excluded from the analysis.

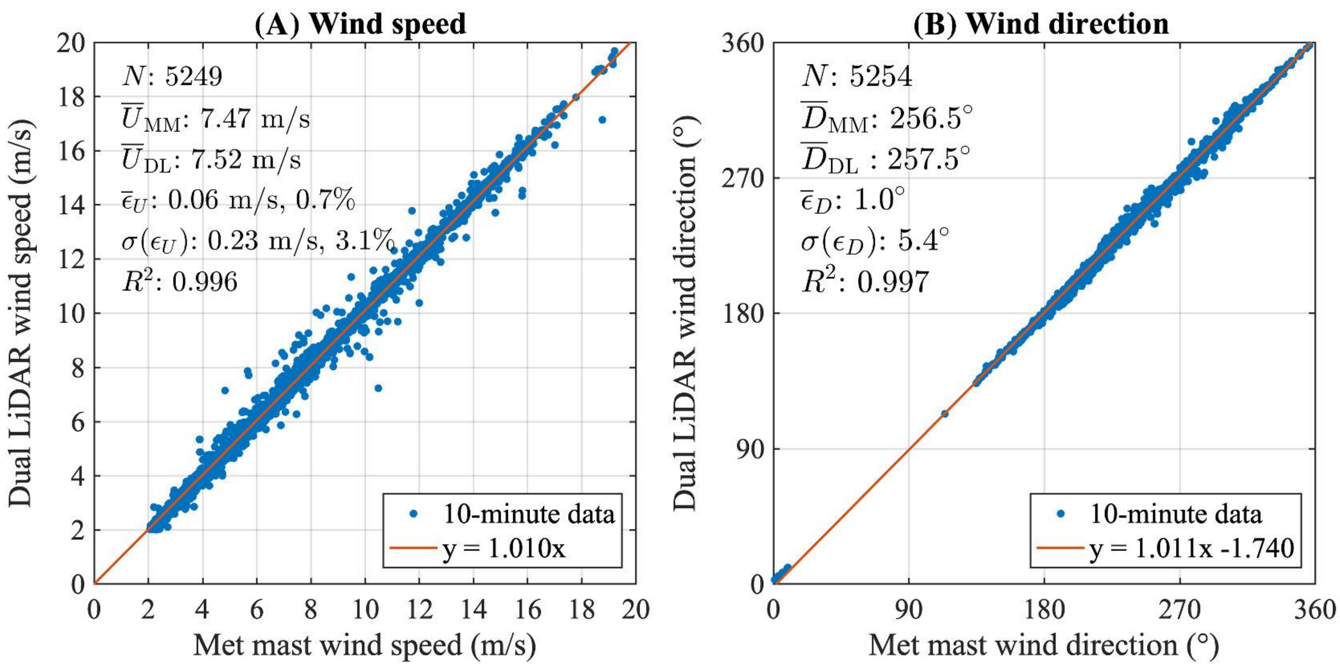

Time series of (A) 10-min mean wind speeds and (B) directions obtained from the met mast (MM) and the dual LiDAR system (DL) for the period November 7 to December 31, 2020

Results – Wind shear and veer

Wind shear and veer

- Above figure shows comparisons of the mean wind speeds obtained from the vertical profiling LiDAR and the dual LiDAR at heights of 66, 120, and 180 m ASL. Dual scanning LiDAR did not depend on the measurement height.

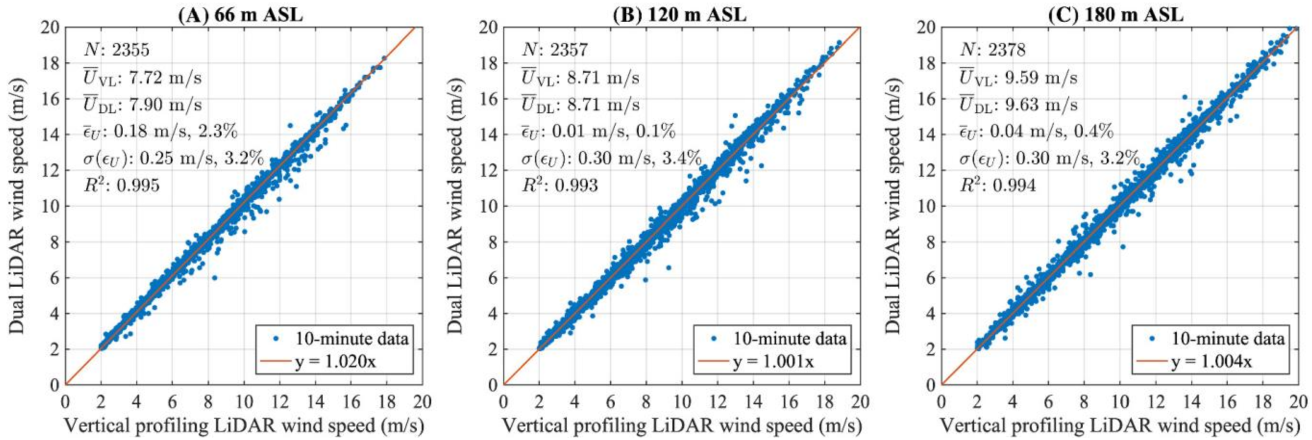

Comparison of 10-min mean wind speeds obtained from the vertical profiling LiDAR device and the dual LiDAR system at heights of (A) 66, (B) 120, and (C) 180 m ASL for the period December 13 to 31, 2020

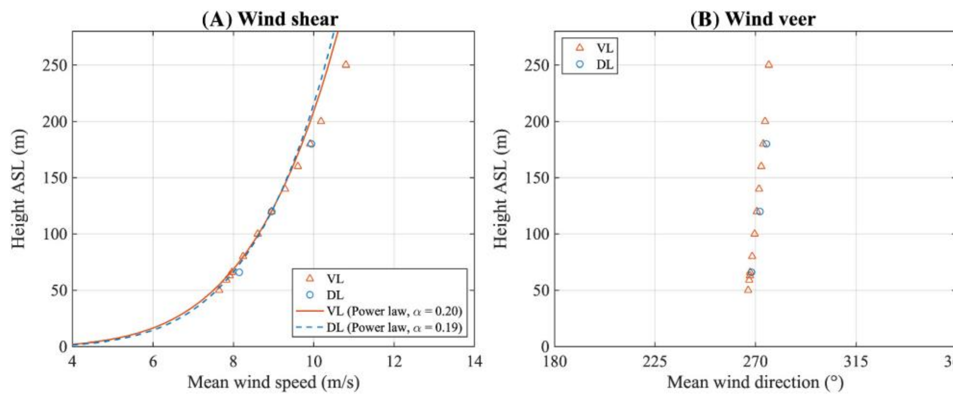

Vertical profiles of (A) mean wind speeds and (B) directions obtained from the vertical profiling light detection and ranging (LiDAR) device (VL) and the dual scanning LiDAR system (DL)

Results – Turbulence intensity [1/2]

- Turbulence intensity
  - Left figures show a scatter plot of the TI, which was obtained from the cup anemometers and SA installed at the met mast versus the DSL.
  - Showing the Right figure, The values from the DSL are found to be slightly higher than those from the cup anemometers at a wind speed range between 2 and 6 m/s; they are **smaller than those from the cup anemometer at a wind speed range of more than 8 m/s**. This small difference would be owing to the difference in measurement principle between the devices.

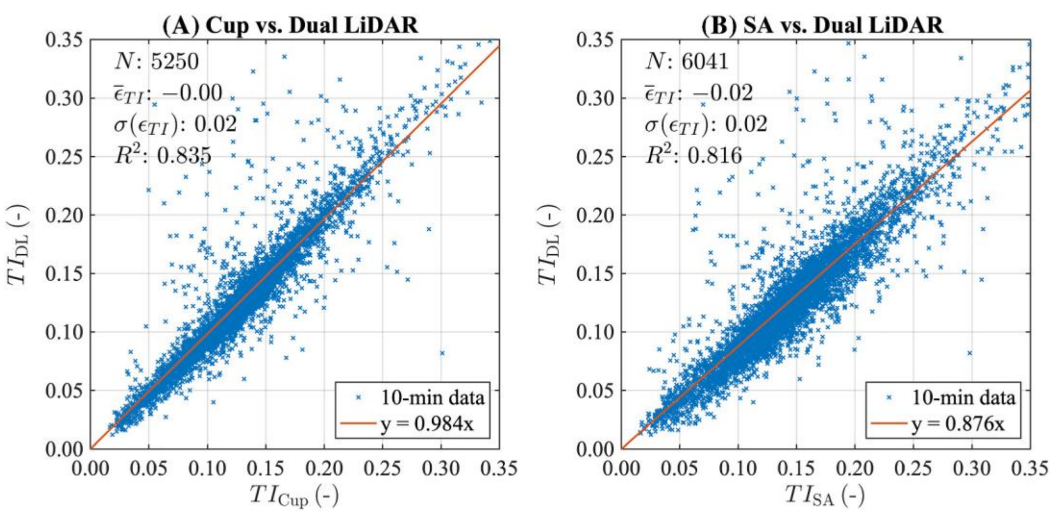

Comparison of TI measured with (A) the cup anemometers and (B) sonic anemometer (SA) at the top of the met mast and the DSL during the experiments for the period November 7 to December 31, 2020

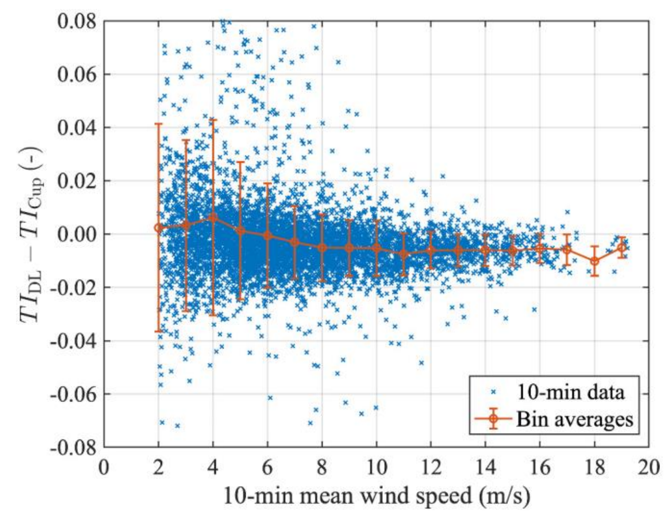

Differences of turbulence intensity measured with the cup anemometers and the DSL as a function of the 10-min mean wind speeds

WINC

Turbulence intensity and number of samples

- Figure (A) shows a comparison of the 90% quantile with a bin width of 0.5 m/s, as obtained from the cup anemometers and the DSL.
- TI obtained from the DSL with the settings used in this study becomes almost equivalent to the TI measured by the cup anemometer, commonly used in wind turbine design.

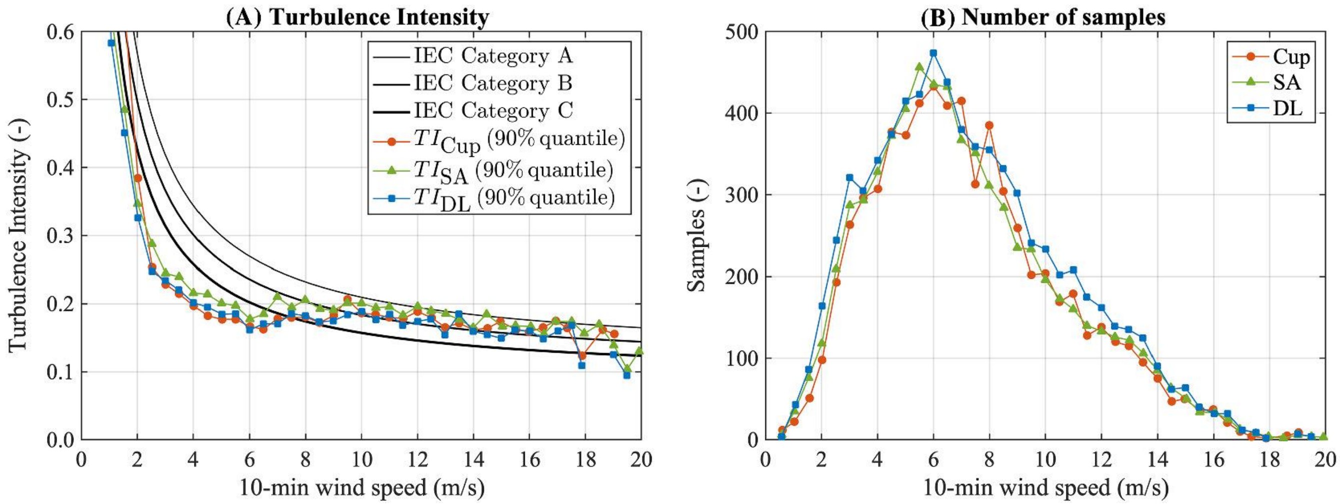

(A) Relationships between 10-min mean wind speed and values for 90% quantile of TI obtained from the cup anemometers, sonic anemometer (SA), and DSL within the wind speed bin of 0.5 m/s. (B) Number of samples included within each bin

Conclusions [1/2]

- The radial velocities
  - **biases of less than 0.2 m/s** and **coefficients of determination of more than 0.99**.

- The 10-min mean wind speed values
  - **mean deviation of +0.06 m/s**, **a standard deviation of deviation of 0.23 m/s**, and a **coefficient of determination of 0.996** against the met mast observations.

- The 10-min mean wind directions
  - **mean deviation of 1.0°**, a **standard deviation of deviation of 5.4°,** and a **coefficient of determination of 0.997**.

- Wind shear and veer
  - Observations from the vertical profiling LiDAR device and the dual scanning LiDAR system had shear exponents of 0.20 and 0.19, respectively.
  - dual scanning LiDAR system did not depend on the measurement height

Conclusions [2/2]

WINC

- Turbulence Intensity
  - Although the relationship of TI measurements from the met mast and the dual LiDAR system was found to be **more scattered than that for the 10-min mean values**, they were still highly correlated.
  - **The 90% quantile obtained from the dual LiDAR system showed almost the same values as those obtained from the cup anemometers**, while they were smaller than the values obtained from the SA. The result of a spectral analysis showed that this difference might be due to the sensitivity of the sensors for measuring atmospheric turbulence.
- The data availability
  - depends crucially on the measurement range. If we consider the dual scanning LiDAR systems as an alternative to installing near-shore met masts for wind measurement, the need to fill in missing data should be considered.
- Calibration
  - calibrating the laser alignment when offshore hard targets are unavailable also needs to be examined.

ACKNOWLEDGEMENTS
This presentation is based on results obtained from a project, JPNP07015, commissioned by the New Energy and Industrial Technology Development Organization (NEDO). The authors are grateful to all the project members associated with the Mutsu-Ogawara validation experiments for their support.